Wind Induced Sediment Resuspension in a Microtidal Estuary

J. G. Booth[1*], R. L. Miller[1], B. A. McKee[2] and R. A. Leathers[1]

[1]National Aeronautics and Space Administration, Earth System Science Office, Bldg. 1100 SA00, Stennis Space Center, MS 39529

[2]Tulane University, Department of Geology, Institute for Earth and Ecosystem Sciences, 208 Dinwiddie Hall, New Orleans, LA 70118

Keywords: Resuspension, Resuspended Sediments, Estuarine Dynamics, Remote Sensing
Regional Terms: USA, Louisiana, Barataria Basin

Abstract

Bottom sediment resuspension frequency, duration and extent (% of bottom sediments affected) were characterized for the fifteen month period from September 1995 to January 1997 for the Barataria Basin, LA. An empirical model of sediment resuspension as a function of wind speed, direction, fetch and water depth was derived from wave theory. Water column turbidity was examined by processing remotely sensed radiance information from visible and near-IR AVHRR imagery. Based on model predictions, wind induced resuspension occurred during all seasons of this study. Seasonal characteristics for resuspension reveal that late fall, winter and early spring are the periods of most frequent and intense resuspension. Model predictions of the critical wind speed required to induce resuspension indicate that winds of 4 m/s (averaged over all wind directions) resuspend approximately 50% of bottom sediments in the water bodies examined. Winds of this magnitude (4 m/s) occurred for 80 % of the time during the late fall, winter and early spring and for approximately 30 % of the time during the summer. More than 50% of the bottom sediments are resuspended throughout the year, indicating the importance of resuspension as a process affecting sediment and biogeochemical fluxes in the Barataria Basin.

---

* Corresponding Author

Introduction

The global flux of river sediment to coastal margins is on the order of 15 x 10^9 t/yr and is largely (> 80%) derived from tropical and subtropical rivers (i.e. between the latitudes of 30°N and 30°S) (Milliman and Meade, 1983; Milliman, 1991). The importance of these sediments in understanding element and pollutant transfer between the continents and oceans is well documented (Meybeck, 1982; Martin and Whitfield, 1987; Martin and Windom, 1991; Valette-Silver et. al., 1993). Coastal sedimentary deposits are a focal site for the biogeochemical transformation of many elements and their study is critical in understanding oceanic elemental mass balances and residence times (Holland, 1978; Berner, 1982; Martin and Windom, 1991). Therefore, knowledge of sediment dynamics in tropical and subtropical estuaries is important for understanding global biogeochemical budgets. However, much of our paradigm for how estuaries process materials is based on studies of temperate coastal environments (Nixon, 1981; Nixson and Pilson, 1983; Kemp and Boynton, 1984; Ward, 1985; Demers and Therriault, 1987; Sanford, 1994; Canuel and Martens, 1996). Fundamental differences exist between these estuarine environments (e.g. estuary type, mixing structure, water depth, tidal influence) that directly affect the way in which tropical and subtropical estuaries process material in comparison to temperate estuaries (Day et al., 1989; Alongi, 1998).

Physical processes (e.g. vertical mixing and sediment resuspension) influence important estuarine parameters such as: primary and secondary productivity, sediment mass flux, and pollutant dispersal. Storms have previously been recognized as important forcing mechanisms for sediment transport in coastal environments (Drake and Cacchione, 1985

and 1986; Cacchione et al., 1987; Roberts et al., 1988; Moeller et al., 1993). In shallow, micro-tidal coastal environments, wind induced waves can be the dominant physical forcing mechanism (Ward, 1980; Solis and Powell, 1999). Mathematical models describing wave formation and propagation have been developed by the U.S. Army Corps of Engineers (Coastal Engineering Research Center (CERC), 1977 and 1984). These models have been evaluated in coastal and lacustrine environments, and the results have been shown to give good agreement with field measurements (Carper and Bachmann, 1984; Schideler, 1984; Demers et al., 1987; Simon, 1989; Arfi et al., 1993).

The study of material transport in coastal environments requires the ability to analyze features which vary dramatically both in time and space. This variability limits the utility of *in situ* measurements for understanding the transfer and processing of materials in coastal margins. However, data obtained from satellites can provide the synoptic information required to study these complex environments (Gorden et al., 1983; Gagliardini et al., 1984; Voillier and Sturm, 1984; and Stumpf, 1988). In particular, data from the National Oceanic and Atmospheric Administration's (NOAA) Advanced Very High Resolution Radiometer (AVHRR) has been applied successfully in the study of coastal sediment dynamics (Stumpf, 1987; Stumpf and Pennock, 1989; Stumpf et al., 1993). The AVHRR is an effective tool for the study of many coastal environments because it provides daily global coverage, it has good radiometric resolution (i.e. ability to distinguish smaller differences in radiance), and it has the dynamic range (i.e., saturation radiance) to study even the most turbid waters (Stumpf, 1987; Gagliardini et al., 1993). The AVHRR instrument has a scanline (swath width) of 2048 pixels, a ground

resolution of 1.1 km and is equipped with 5 spectral bands, 1 visible channel and 4 infrared channels.

Here we combine a wind driven resuspension model with remote sensing techniques to characterize sediment resuspension in the Barataria Basin, LA.

Study Area

General Description

The Barataria Basin is an interdistributary estuarine-wetland system located in southeast Louisiana (Fig. 1). It is bordered on the north and east by the Mississippi River and on the west by Bayou Lafourche. The basin has a total area of approximately 628,000 hectares (ha), including 202,000 ha of open water and 206,000 ha of marsh (Fig. 2; Conner and Day, 1987). Dominant morphological features include levees (natural and artificial), canals, bayous, bays, lakes, swamp and marsh wetlands, and barrier islands (Conner and Day, 1987). The Barataria estuary may be characterized as a bar-built lagoon; it is shallow with sandbars at the mouth and has a small tidal range (Adams et al., 1976). The average depth of open water bodies is approximately 2 meters (Conner and Day, 1987). Tides in the basin are diurnal with an average range of 32 cm at the coast (Baumann, 1987). On average, coastal Louisiana receives about 160 cm of precipitation annually (Baumann, 1987). Presently, the basin is experiencing reduced freshwater input (due to leveeing of the Mississippi River and surrounding waterways), increasing salinity and wetland erosion, resulting in a rapid transition back to an open marine environment (Madden et al., 1988).

Climate

The climate of the Barataria is largely controlled by its subtropical location and proximity to the Gulf of Mexico (Sanders, 1978). Seasonal weather patterns for coastal Louisiana are primarily influenced by two pressure systems; the Bermuda High and the Mexican Heat Low (Leipper, 1954; Baumann, 1987). The Bermuda High is located over the Bermuda-Azores area of the western Atlantic and is weakened and in a northerly location during the winter, and strengthened and in a southerly location during spring and summer (Schroeder and Wiseman, 1999). The Mexican Heat Low is located over Texas and is well established during the summer (Baumann, 1987). The position and relative strength of the Bermuda High imparts a steering effect on high pressure systems advancing southward over the conterminous U.S., and ultimately determines the orientation and southern extent of a front as it crosses coastal Louisiana. The Mexican Heat Low influences the speed and direction of southerly dominant winds, during the summer months, due to its position and strength. Therefore, during winter northerly winds are dominant with northeasterly winds occurring most frequently whereas, during the summer southerly winds become dominant with southeasterly winds occurring most frequently (Baumann, 1987).

Hydrology

The Barataria Basin is a meteorologically forced, micro-tidal estuary (Boesch et al., 1989). Water movement through the basin is a function of tidal influence, winds and precipitation. The combination of these influences creates slow moving bayous and promotes sheet flow over the wetlands (Conner and Day, 1987). Seasonal water level in

the basin exhibits a bimodal distribution with maximum water levels occurring in the spring, due to precipitation and runoff, and summer, due to an expanding Gulf water mass (Baumann, 1987). The spring peak is discernable but considerably attenuated for locations in the lower basin. This is attributed to a decreased upland runoff influence (marine dominance) for the lower basin (Baumann, 1987).

The natural hydrology of the basin has been altered extensively by human activities such as, channel dredging and levee construction (Turner and Cahoon, 1988). For example, leveeing of the Mississippi River has effectively eliminated the major fluvial input of freshwater and sediments to the basin. Precipitation is now the primary source of freshwater. Linear canals dredged to depths greater than the surrounding bay bottoms promote the intrusion of high salinity water into the interior basin, and also provide efficient conduits for the transport of materials out of the basin. The overall effect of these activities has been to decrease the transfer of sediments to the marsh surface, thereby decreasing the sustainable marsh area of the basin.

Material Transport

The transfer of material (e.g. silt, clay, organic matter and nutrients) within the basin depends on water movement. Before the river was leveed, the bulk of material transport occurred in the spring in relation to the annual Mississippi River flood. Presently, maximum water exchange in the Barataria occurs in the fall and winter in response to the passage of cold fronts (Baumann, 1987; Madden et al., 1988). During these seasons an average of over 5 frontal passages occur per month (Baumann, 1987). As a cold front

approaches the coast, southerly component winds strengthen and push water into the basin, flooding the marshes. After the front passes, northerly component winds become dominant and push the water out of the basin, draining the marshes. Water level variability in the marsh approaching 1m d^{-1} has been documented in relation to wind stress (Muller, 1979). This scenario is repeated for each frontal passage and has been shown to be important for material transport in the basin. Storm passages are now the only mechanism that transports sediments to the surface of the marsh. A study of the seasonality of marsh accretion indicates that as much as 75% of the annual accretion results from winter storm passages, in years when tropical storms did not impact the basin (Baumann et al., 1984). The source of these sediments is primarily resuspended bottom sediments from lakes and bays (Madden et al., 1988).

Theory

Predicting Resuspension from Wind-Induced Waves

Surface waves are produced when wind blows across a body of water. A wave traveling in water with a depth (d) that is greater than one-half the wavelength (L) is classified as a deepwater wave (Pond and Pickard, 1983). As a deepwater wave propagates, surface water particles move in an approximately circular path (Fig 3). The radius of this path decreases exponentially with depth, approaching zero at L/2 (Pond and Pickard, 1983). When $d < 1/2L$, the wave motion reaches the bottom and the wave transfers energy to the bottom sediments, possibly causing resuspension. Therefore, wavelength (L) is the

critical parameter for characterizing resuspension for a given water body. Wavelength is related to wave period by

$$L = gT^2/2\pi, \tag{1}$$

where g is gravitational acceleration (9.8 m s^{-2}) and T is the wave period (CERC, 1984). The period of wind induced waves is determined primarily by wind velocity, wind fetch and wind duration. If 24 hour resultant wind vectors are used, then T can be predicted from the wind velocity (U) and fetch (F) given that (CERC, 1984)

$$gT_m/U_A = 0.2857(gF/U_A^2)^{1/3}, \tag{2}$$

where U_A is a wind stress factor and is determined from

$$U_A = 0.71(UR_T)^{1.23}. \tag{3}$$

R_T is a boundary layer stability correction factor, which is dependent on the temperature difference between the water and air and is expressed as

$$R_T = f(T_a - T_s), \tag{4}$$

where T_a and T_s represent the temperature of the air and surface water. When temperature information is not available a value of 1.1 is recommended for R_T (CERC, 1984).

Remote Sensing of Suspended Sediments

The optical properties of water, in the visual portion (400 – 700 nm) of the electromagnetic spectrum, result from the concentrations of suspended and dissolved constituents in the water column. A quantitative application of remote sensing to the study of ocean optics requires an understanding of how the total spectral signal measured at a remote instrument can be partitioned into water-leaving and non water-leaving components. The total radiance (L_t) measured at the sensor can be written as

$$L_t(\lambda) = L_A(\lambda) + tL_w(\lambda) + L_{sg}(\lambda), \quad (5)$$

where t is the diffuse transmittance of the light through the atmosphere, λ is the sensor band or wavelength, L_w is the water-leaving radiance, L_A is the radiance attributed to atmospheric scattering, and L_{sg} is the radiance attributed to sunglint from surface water. It is the water-leaving component that contains information on the water constituents, while the non water-leaving component is related to viewing the water through the atmosphere.

By avoiding regions of an image that contain sunglint, L_{sg} can be omitted from equation 5. The atmospheric path radiance (L_A) is estimated by applying the clear water subtraction technique (Gordon et. al., 1978). This technique utilizes the fact that clear water is a strong absorber of long wavelength energy (e.g. red and near-IR regions) and in the absence of suspended particulates, $L_w = 0$. Therefore, the radiance values measured in these regions of the electromagnetic spectrum are due to atmospheric

scattering. The concentration and size distribution of aerosol particles is assumed constant over the entire scene and the clear water radiance representative of the atmospheric component at all wavelengths (Stumpf, 1987). The water-leaving radiance can be extracted from the total radiance (L_t (λ)) by rearranging equation 5,

$$L_w(\lambda) = \{(L_t(\lambda) - (L_A(\lambda))\} / t(\lambda). \quad (6)$$

However, L_w is not an accurate indicator of water properties as it is influenced as much by the incident solar irradiance as the water quality (Robinson, 1985). By normalizing the radiance measured at the satellite for the incident light field at the ocean surface (E_d), we obtain remote sensing reflectance

$$R_{RS}(\lambda) = L_w(\lambda)/E_d(\lambda), \quad (7)$$

which is directly related to water turbidity (Stumpf, 1987). E_d is calculated by propagating the solar irradiance at the top of the atmosphere (E_o) to the ocean surface by correcting for the sun's altitude and the Earth – Sun distance, and is given by $E_d = E_o \cos \theta_o$, where $E_o = \underline{E}_o [1 + 0.0167 \cos [2\pi(D-3)]^2$, D is the Julian day of data collection, $\underline{E}_o$ is the mean solar constant and θ_o is the solar zenith angle (Stumpf, 1987). Therefore,

$$R_{RS}(\lambda) = L_w(\lambda)/E_o(\lambda) \cos(\theta_o)\ T_1, \quad (8)$$

where atmospheric attenuation of E_o (from the sun to the earth) is represented by T_1.

Methods

Seasonal Turbidity via Remote Sensing

AVHRR level 1b Local Area Coverage (LAC) and High Resolution Picture Transmission (HRPT) imagery was obtained from the NOAA Satellite Active Archive (http://sit.saa.noaa.gov/). Channel 1 and 2 data for images that contained little or no cloud cover in the study region were processed and analyzed using the *ENVI* (Research Systems, Inc., Boulder, CO) software package. The radiances were georeferenced and converted to percent reflectance using a one-step algorithm (Di and Rundquist, 1994). This algorithm applies the auxiliary parameters (e.g. calibration coefficients, Earth location, solar-zenith angles) appended to level 1b data to remove geometric and radiometric errors. The calibrated reflectances were used to calculate the remote sensing reflectance of Eq. (8). The atmospheric transmissions t and T_1 were taken to be unity, which leads to R_{RS} values that are underestimates of the true reflectance. In this study we are interested only in the relative differences in reflectance values among the pixels in a particular scene, and therefore, the actual values of t and T_1 are not important. The clear water reflectance was subtracted from the total reflectance R_t of each pixel in the scene. The resulting quantity is

$$R_{RS} = (R_t - R_{tc})/E_o \cos \theta_o, \qquad (9)$$

where R_{tc} represents the total reflectance measured over clear water.

Wind Characteristics

Hourly wind data (direction and speed) were obtained from the NOAA National Data Buoy Center (NDBC) (http://seaboard.ndbc.noaa.gov/) meteorological buoy located just south of Grand Isle, Louisiana (buoy ID = GDIL1). The data were normalized to wind speeds 10 meters above the sea surface using

$$U(10m) = U(z)\ (10/z)^{1/7}, \tag{10}$$

where U represents wind speed in m/s and z represents the height above sea surface that the winds were measured (CERC, 1984). This equation is valid for winds measured over water when $z \leq 20$ meters (CERC, 1984). The normalized wind data were used to characterize seasonal winds and to drive the resuspension model. Wind data were divided into 10 periods covering the time frame from Sept. 23, 1995 to Jan. 4, 1997. These periods were further grouped into seasons: fall and winter encompassed September through February; spring included March through May; while summer included the months of June through August.

Modeling Wind-Induced Resuspension

A computer program was written to calculate fetch (F), critical wind speed (U_c), wavelength (L) and wave period (T) across a body of water, for winds of any speed blowing from the eight compass directions as defined in Figure 4. Navigation charts were digitized to provide shoreline boundaries and bathymetry for the program. A file of each of the model parameters was generated for each program run. These files were

imported into ENVI for processing and visualization. The following parameters were calculated from equations 1 and 2 above:

T_c (critical wave period) = $(4\pi d/g)^{1/2}$

U_c (critical wind speed) = $[1.2\{4127(T_c^3/F)\}^{0.813}]$

T (significant wave period) = $[0.2857(gF)^{1/3} U_A^{1/3}]/g$

L (wavelength) = $gT^2/2\pi$

RP (resuspension potential) = $U - U_c$.

Resuspension Model Validation

Because no *in situ* turbidity measurements were available to check the validity of the resuspension model, we compared reflectance values from the satellite imagery to model predictions of resuspension potential. Thus, an image of U_c for a water body, corresponding to the wind characteristics from a given day, was compared to the AVHRR image collected on the same day. Specifically, the 24 hour resultant wind vector was calculated for a given day that a useable (i.e. cloud free) AVHRR image was available. This wind data was used for the model run. The model output image for U_c was resampled to 1km resolution to permit a direct comparison with the satellite imagery. Corresponding transects were then subsampled to obtain U_c and reflectance data. The U_c data were then subtracted from the mean wind speed (U) for that day to produce the RP parameter. The model was validated using data from Lake Pontchartrain because advective inputs to the lake were minimal compared to water bodies within the Barataria Basin (advective inputs will tend to skew the reflectance data either higher or lower

depending on the source of the advected waters). Lake Pontchartrain is a large (1645 km^2), shallow (average depth is 4 m) water body located on the northern boundary of the study area and is hydrologically isolated (i.e. the majority of suspended material in the water column is generated from within the lake) in comparison to the open water bodies within the Barataria Basin.

Results and Discussion

Seasonal Wind Forcing

Wind data exhibited expected trends, with the strongest winds occurring in the fall, winter and early spring in conjunction with cold front passages. Mean daily wind speeds ranged from 5.7 m/s in the fall to 2.8 m/s in the summer (Figure 5). Northerly component winds (i.e. winds from the NW, N and NE) were always stronger than southerly component winds (i.e. winds from the SW, S and SE), with the exception of late spring and summer (Figure 5). During fall and winter northerly component winds were dominant and averaged 6.5 m/s, while southerly component winds averaged 3.6 m/s (Figure 5). However, during summer months southerly component winds became dominant and averaged 2.9 m/s, while northerly component winds averaged 1.8 m/s (Figure 5).

The directional distribution of wind energy (U^2) for this study (Table 1) reveals that northerly component winds were the primary forcing agent, accounting for 58% of the total wind energy; while southerly component winds contributed 26% of the wind energy.

A seven year average for directional wind energy distribution (Table 2) returned values of 52% and 26% for northerly and southerly component winds. Therefore, it appears that for a typical year the net transfer direction for water-borne materials (i.e. dissolved and particulate materials) should be southerly. Ultimately, what controls the affect of these northerlies on the basin, for a given year, are the characteristics of cold front passages (i.e. orientation to the coastal environment, strength, speed and direction of propagation). However, in years when a tropical storm or hurricane impacts the basin, the directional wind energy distribution could be significantly influenced (i.e. depending on the path of the system).

Resuspension Model Results

For a given scenario of wind speed, direction and fetch over water, as the resuspension potential increases above the value of zero, a concomitant increase in water column turbidity, here measured as reflectance, should result. Model estimates of resuspension potential (RP) show good agreement with satellite reflectance data (Figure 6) for Lake Pontchartrain. The covariance between RP and % reflectance indicates that the model prediction of when resuspension should occur is reasonable.

Model estimates of U_c for Lake Salvador, Little Lake and the lower Barataria Basin were calculated for each of the eight wind directions indicated in Figure 4. Contour plots of U_c for due north and south winds for each water body are depicted in (Figures 7 - 9). Because of the shallow nature of these water bodies, areas of resuspension are primarily determined by the fetch. Therefore, critical windspeeds are high near the windward

shores of the water bodies and low near the leeward shores. Areal estimates of bottom sediment resuspension are given as a function of wind speed and direction in Tables 3, 4 and 5 for the same water bodies.

Seasonal Resuspension Characteristics

From the characterization of winds during each period of this study and model estimates of U_c, we can begin to quantify the characteristics of resuspension (i.e. frequency, duration and areal extent) in the Barataria Basin. During the fall, winter and early spring (i.e. periods 1 – 4, 9 and 10) northerly component winds accounted for more than 65% of the wind energy during each period (Table 1). These periods also exhibited the highest mean daily wind speeds for this study (Figure 5). Areal resuspension estimates (Tables 3, 4 and 5) indicate that the windspeed necessary to affect 50% of bottom sediments in each water body, is 4 m/s. The region affected is much smaller for lower windspeeds. For northerly component winds of 4 m/s, more than 50% of bottom sediments in each water body were subject to resuspension, primarily on the southern side (Figs. 7, 8, and 9). During spring and summer (i.e. periods 5 – 8) southerly component winds accounted for more than 50 % of the wind energy during each period (Table 1). However, these periods exhibited the lowest mean daily wind speeds for this study (Figure 5). Areal resuspension estimates (Tables 3, 4 and 5) indicate that for southerly component winds of 4 m/s, over 45 % of bottom sediments in each water body were subject to resuspension, primarily on the northern side (Figs. 7, 8 and 9). During summer months, (periods 7 and 8) west and east winds contributed significantly to the total wind energy; west winds accounted for approximately 20 % of wind energy during period 7, while east winds

accounted for approximately 30 % of the wind energy during period 8 (Table 1). Again, areal bottom sediment resuspension estimates in Tables 3, 4 and 5 indicate that greater than 55 % of bottom sediments, in each water body, were subject to resuspension for easterly or westerly winds of 4 m/s. Winds of this magnitude (4 m/s) occurred during all periods of this study; and indicate that significant resuspension events should occur throughout the year as well. However, fall, winter and early spring appear to be the times when resuspension is most intensive (i.e. highest wind speeds) and frequent (i.e. wind speeds were greater than 4m/s approximately 80 % of the time) (Figure 10). In contrast, summer appears to be a time of lower resuspension intensity (i.e. lowest wind speeds) and lower frequency (i.e. wind speeds were greater than 4 m/s approximately 35 % of the time) (Figure 10). However, it should be noted that the frequency of thunderstorm occurrence is at a maximum during summer months (Hopkinson et. al., 1985), and because of their limited spatial influence most of these thunderstorms are not included in the wind data utilized for this study.

Seasonal Deposition

In conjunction with the water column resuspension work presented here, seasonal rates of deposition and erosion of particulate material to bottom sediments were investigated (Booth et al., 1999). By utilizing a naturally occurring radioisotope (i.e. ^{7}Be) as a tracer of particulate material, Booth et. al., 1999 quantified rates of net particle deposition and erosion at two contrasting sites, Little Lake (LLN) and Live Oak Bay (LOB), in the lower basin. The LLN station was located in a shallow (~ 1.5 m), large (~ 114 km^2) lake and was unprotected from wind exposure (i.e. large fetch). In contrast, the LOB station was

located in a shallow (~ 1 m depth), small (~ 1 km^2) water body which was adjacent to the littoral edge of the surrounding wetlands, and more protected from wind exposure (i.e. small fetch). Sources of particulate material to the LLN station would include resuspended sediments from Little Lake as well as from water bodies north and south of the lake depending on the duration and strength of prevailing winds. Sediment sources to the LOB site include material from the surrounding marshes as well as resuspended sediments from water bodies south of the station (e.g. Hackberry Bay and Barataria Bay).

Particle deposition occurred throughout the study period (15 months) at each station (Figure 11). The annual deposition measured at the LLN site was primarily accounted for during two periods of contrasting winds, periods 5 and 9. In period 5 an abrupt shift from northerly to southerly dominant winds occurred (Table 1) resulting in the highest rate of sediment deposition measured at the LLN site (Figure 11). In contrast, during period 9 winds shifted from southerly to northerly dominant (Table 1) resulting in an intense erosional period (Figure 11). Spring and summer accounted for 75% of the net sediment deposition which occurred at the LLN site. The annual deposition measured at the LOB site was primarily accounted for during the fall, winter and early spring, periods 1 through 4. During these periods, greater than 60% of the net sediment deposition for the 15 month study was accounted for (Figure 11), and winds were primarily from the north (Table 1).

The results derived from a combination of radioisotope, remote sensing and modeling techniques indicate that the annual transport of sediments (i.e. resuspension,

redistribution and deposition) in the Barataria Basin varies seasonally. Down basin transport dominates during the cold front season (i.e. fall, winter and early spring) and up basin transport dominates during the late spring and summer. Further, sedimentation at any site will vary in relation to the orientation with the dominant winds and the size of the water body.

Summary

Data and results presented here indicate the following:

Model predictions of sediment resuspension in Lake Pontchartrain (estimated from wind speed information and models of wind induced wave characteristics) show good agreement with surface water reflectance (i.e. turbidity) derived from satellite imagery. Based on this validation the seasonal characteristics of resuspension for the Barataria Basin were described.

Bottom sediment resuspension occurs throughout the year in the Barataria Basin. Annual characteristics for resuspension indicate that in fall, winter and early spring resuspension events are most frequent (mean wind speeds averaged ~ 5 m/s) and intensive (dominant wind speeds averaged ~ 6.5 m/s). Northerly component winds are dominant during these times and result in the down basin transfer of water and suspended materials. In contrast, late spring and summer exhibit less frequent (mean wind speeds averaged < 3 m/s) and less intensive (dominant wind speeds averaged ~ 3 m/s) resuspension events. However,

southerly component winds dominate during these time periods and result in an up basin transport of water and suspended materials. Thunderstorms occur with the highest frequency during the summer months and likely result in localized affects of resuspension and redistribution, as compared to the basin wide transport mentioned above.

Areal estimates of bottom sediment resuspension (based on contour plots of critical wind speed) indicate that northerly or southerly component winds of 4 m/s resuspend approximately 50 % of bottom sediments in Lake Salvador, Little Lake and the lower Barataria Basin. Winds of this magnitude occur most frequently during the fall and winter (i.e. > 80 % of the time), and least frequently during late summer (< 30% of the time). Areal resuspension estimates indicate that at winds of 10 m/s greater than 80 % of bottom sediments experience wave induced resuspension in the water bodies examined here.

Acknowledgements

The authors thank Jason Hasenbuhler, for writing the code for the resuspension model and Lloyd McGregor, for digitizing navigational charts.

REFERENCES

ADAMS, R. D., BARRETT, B. B., BACKMON, J. H., GANE, B. W. AND MCINTIRE, W. G. 1976. Barataria Basin: geologic processes and framework. Louisiana State University, Center for Wetland Resources, Baton Rouge. Sea Grant Publ. No. LSU-T-76-006.

ALONGI, D.M. 1998. *Coastal Ecosystem Processes*. CRC Press, Boca Raton, pp. 420.

ARFI, R., GUIRAL, D., AND BOUVY, M. 1993. Wind induced resuspension in a shallow tropical lagoon. *Estuarine Coastal Shelf Sci.* 36: 587-604.

BAUMANN, R. H. 1987. Physical Variables. *In*: The ecology of Barataria Basin, Louisiana: An estuarine profile. (eds. W.H. Conner and J.W. Day, Jr.) U.S. Fish and Wildlife Service, Biological Report 85 (7.13) pgs. 8-17.

BAUMANN, R. H., DAY, J. W, JR. AND SMITH, C. A. 1984. Mississippi deltaic wetland survival: Sedimentation vs coastal submergence. *Science,* 224:1093-1095.

BERNER, R. 1982. Burial of organic carbon and pyrite in the modern ocean: its geochemical and environmental significance. *Am. J. Sci.,* 282: 451-473.

BOESCH, D. F., DAY, J. W., JR. AND CONNER, W. 1989. The Barataria-Terrebonne estuarine complex. *In*: Governor's nomination and request for a management conference under the National Estuary Program. 109 pgs.

BOOTH, J.G., MCKEE, B.A. AND MERIWETHER, J.R. 1999. The transport and fate of particulate material in a shallow, turbid estuary: Seasonal and decadal characteristics from ^{7}Be and ^{210}Pb techniques. *Geochem. Cosmochim. Acta.* (submitted).

BOYNTON, W. R., KEMP, W.M., AND OSBORNE, C.G. 1980. Nutrient fluxes across the sediment-water interface in the turbid zone of a coastal plain estuary. *In*: V. Kennedy (ed.) Estuarine Perspectives. Academic Press, New York. pp. 93-109.

CACCHIONE, D.A., GRANT, W.D., DRAKE, D.E. AND GLENN, S.M. 1987. Storm-dominated bottom boundary layer dynamics on the northern California continental shelf: Measurements and Predictions. *J. Geophys. Res.,* 92:1817-1827.

CANUEL, E.A. AND MARTENS, C.S. 1996. Reactivity of recently deposited organic matter: Degradation of lipid compounds near the sediment-water interface. *Geochim. Cosmochim. Acta,* 60: 1793-1806.

CARPER, G.L. AND BACHMANN, R.W. 1984. Wind resuspension of sediments in a prairie lake. *Can. J. Fish. Aquat. Sci.,* 41: 1763-1767.

CONNER, W.H. AND DAY, J.W. (eds) 1987. *The ecology of Barataria Basin, Louisiana: An estuarine profile.* U.S. Fish and Wildlife Service, Biological Report 85(7.13), 166pp.

DAY, JR., J.W., HALL, C.A.S., KEMP,W.M. AND YANEZ-ARANCIBIA, A. 1989. *Estuarine Ecology.* John Wiley & Sons, New York, 558 pp.

DEMERS, S. AND THERRIAULT, J-C. 1987. Resuspension in the shallow sublittoral zone of a macrotidal estuarine environment: Wind influence. *Limnol. Oceanogr.*, 32 (2): 327-339.

DI, L. AND RUNQUIST, D.C. 1994. A one step algorithm for correction and calibration of AVHRR level 1b data. *Photogrammetric Engineering and Remote Sensing,* 60: 165-171.

DRAKE, D.E. AND CACCHIONE, D.A. 1985. Seasonal variation in transport on the Russian River Shelf, California. *Cont. Shelf Res.,* 4:495-514.

DRAKE, D.E. AND CACCHIONE, D.A. 1986. Field observations of bed shear stress and sediment resuspension on continental shelves, Alaska and California. *Cont. Shelf Res.,* 6:415-429.

GAGLIARDINI, D.A., KARSZENBAUM, H., LEGECKIS, R. AND KLEMAS, V. 1984. Application of Landsat MSS, NOAA/TIROS AVHRR, and Nimbus CZCS to study the La Plata River and its interaction with the ocean. *Remote Sensing of Environment,* 15:21-36.

GORDON, H.R. 1978. Removal of atmospheric effects from satellite imagery of the oceans. *Applied Optics,* 17: 1631-1636.

GORDON, H.R., CLARK, D.K., BROWN, J.W., BROWN, O.B., EVANS, R.H., AND BROENKOW, W.W. 1983. Phytoplankton pigment concentrations in the Middle Atlantic Bight: Comparison of ship determinations and CZCS estimates. *Applied Optics.* 22: 20-33.

HOLLAND, H. D. 1978. The chemistry of the atmosphere and oceans, 351 pp, Wiley Interscience, New York.

HOPKINSON, C. S., DAY, J.W. JR. AND KJERFVE, B. 1985. Ecological significance of summer storms in shallow water estuarine systems. *Contributions in Marine Science,* 28:69-77.

KEMP, W.M. AND BOYNTON, W.R. 1984. Spatial and temporal coupling of nutrient inputs to estuarine primary production: the role of particulate transport and decomposition. *Bull. Mar. Sci.* 35:522-535

LEIPPER, D.F. 1954. Marine meteorology of the Gulf of Mexico, a brief review, pp. 89-98. *In*: Gulf of Mexico, its origin, waters, and marine life. Bull. Fish. Wild. Ser. 55.

MADDEN, C. J., DAY, J. W., JR. AND RANDALL, J. M. 1988. Freshwater and marine coupling in estuaries of the Mississippi River deltaic plain. *Limnol. Oceanogr.*, 33: 982-1004.

MARTIN, J.-M. AND WINDOM, H.L. 1991. Present and future roles of ocean margins in regulating marine biogeochemical cycles of trace elements. *In*: Ocean Margin Processes in Global Change. (Eds. R.F.C. Mantoura, J.-M. Martin and R. Wollast.) pp. 45-68, John Wiley and Sons, Chichester.

MARTIN, J.-M. AND WHITFIELD, J. 1983. The significance of the river input of chemical elements to the ocean. *In*: Trace Metals in Seawater, ed. C.S. Wong, E. Boyle, K.W. Brulend, J.D. Burton, and E.D. Goldberg. NewYork and London: Plenum.

MARTIN, J.-M. AND MEYBECK, M. 1979. Elemental mass balance of material carried by major world rivers. *Mar. Chem*, 7: 173-206.

MEYBECK, M. 1982. Carbon, nitrogen and phosphorus transport by major world rivers. *Am. J. Sci.*, 282: 401-450.

MILLER, R.L., CRUISE, J.F., OTERO, E. AND LOPEZ, J.M. 1994. Monitoring suspended particulate matter in Puerto Rico: Field measurements and remote sensing. *Water Resources Bulletin.* 30 #2: 271-282.

MILLIMAN, J.D. 1991. Flux and fate of fluvial sediment and water in coastal seas. *In*: Ocean Margin Processes in Global Change (Eds. R.F.C. Mantoura, J.-M. Martin and R. Wollast.), pp. 69-90, John Wiley and Sons, Chichester.

MILLIMAN, J.D. AND MEADE, R.H. 1983. World-wide delivery of river sediment to the oceans. *J. Geol.* 91:1-21.

MOELLER, C., HUH O., ROBERTS, H., GUMLEY, L. AND MENZEL, P. 1993. Response of the Louisiana coastal environments to a cold front passage. *J. Coast. Res.* 9: 434-447.

MULLER, R. A. 1979. Some environmental responses to synoptic weather type regimes in southern Louisiana. In: Coastal marsh and estuary management, Proc. 3rd Symp. Louisiana State University. Pgs. 165-189.

NECKEL, H. AND LABS, D. 1984. The solar radiation between 3300 and 12500 *A. Solar Physics,* 90:205-258.

NIXON, S.W. 1981. Remineralization and nutrient cycling in coastal marine ecosystems. Pp. 111-138. In: E. Carpenter and D. Capone (eds.) *Estuarine and Nutrient.* Humana Press. Clifton, NJ.

NIXON, S.W. AND PILSON, M. 1983. Nitrogen in estuarine and coastal marine ecosystems; pp. 565-648. *In*: E. Carpenter and D. Capone (eds.), Nitrogen in the Marine Environment. Academic Press, New York.

POND, S. AND PICKARD, G.L. 1983. Introductory Dynamical Oceanography. Pergamon Press, pp. 329.

ROBERTS, H.H., HUH, O.H., HSU, S.A., ROUSE, L.J. AND RICKMAN, D. 1988. Impact of cold-front passages on geomorphic evolution and sediment dynamics of the complex Louisiana coast. Pp. 1950 – 1963. *In*: Coastal Sediments '87, Proceedings of a Specialty Conference, American Society of Civil Engineers.

ROBINSON, I.S. 1985. *Satellite Oceanography.* John Wiley & Sons, New York. Pp. 455

SANFORD, L. P. 1994. Wave-forced resuspension of upper Chesapeake Bay muds. *Estuaries*, 17(1B): 148-165.

SHIDELER, G.L. 1984. Suspended sediment responses in a wind-dominated estuary of the Texas Gulf coast. *J. Sed. Petrol.*, 54: 731-745.

SIMON, N.S. 1989. Nitrogen cycling between sediment and the shallow-water column in the transition zone of the Potomac River Estuary: The role of wind-driven resuspension and adsorbed ammonium. *Estuar. Coast. Shelf Sci.*, 28: 531-547.

STUMPF, R.P. 1987. Application of AVHRR satellite data to the study of sediment and chlorophyll in turbid coastal waters. NOAA technical memorandum, NESDIS AISC 7, 50 pp.

STUMPF, R.P. 1988. Sediment transport in Chesapeake Bay during floods: analysis using satellite and surface observations. *J. Coastal Research* 4: 1-15.

STUMPF, R.P. AND PENNOCK, J.R. 1989. Calibration of a general optical equation for remote sensing of suspended sediments in a moderately turbid estuary. *J. Geophys. Res.*, 94:14363-14371.

STUMPF, R.P., GELFENBAUM, G. AND PENNOCK, J. R. 1993. Wind and tidal forcing of a buoyant plume, Mobile Bay, Alabama. *Cont. Shelf Res.*, 13 #11:1281-1301.

TURNER, R. E. AND CAHOON, D. R. 1988. Causes of wetland loss in the coastal central Gulf of Mexico. U.S. Dept. of the Interior, Minerals Management Service, Gulf of Mexico. OCS Regional Office. OCS Study MMS 87-0119.

U.S. ARMY COASTAL ENGINEERING RESEARCH CENTER (CERC). 1977. Shore protection manual. Vol. 1: 3rd Edition, pp. U.S. Army Coastal Engineering Center, Fort Belvoir, VA.

U.S. ARMY COASTAL ENGINEERING RESEARCH CENTER (CERC). 1984. Shore protection manual. Vol. 1:4th Edition, pp. 603, U.S. Army Coastal Engineering Center, Fort Belvoir, VA.

VALETTE-SILVER, N.J., BRICKER, S.B., AND SALOMONS, W. 1993. The use of sediment cores to reconstruct historical trends in contamination of estuarine and coastal sediments. *Estuaries*, 16(3B): 577-588.

VOILLIER, M. AND STURM, B. 1984. CZCS data analysis in turbid coastal water. *J. Geophys. Res.*, 89 #D4: 4977-4985.

WARD, G.H., Jr. 1980. Hydrography and circulation processes of Gulf estuaries, p. 183-215. In: P. Hamilton and K.B. MacDonald (eds.), *Estuaries and wetland processes with emphasis on modeling*, Plenum Press.

WARD, L. G. 1985. The influence of wind waves and tidal currents on sediment resuspension in middle Chesapeake Bay. *Geo-Marine Letters,* 5: 71-75.

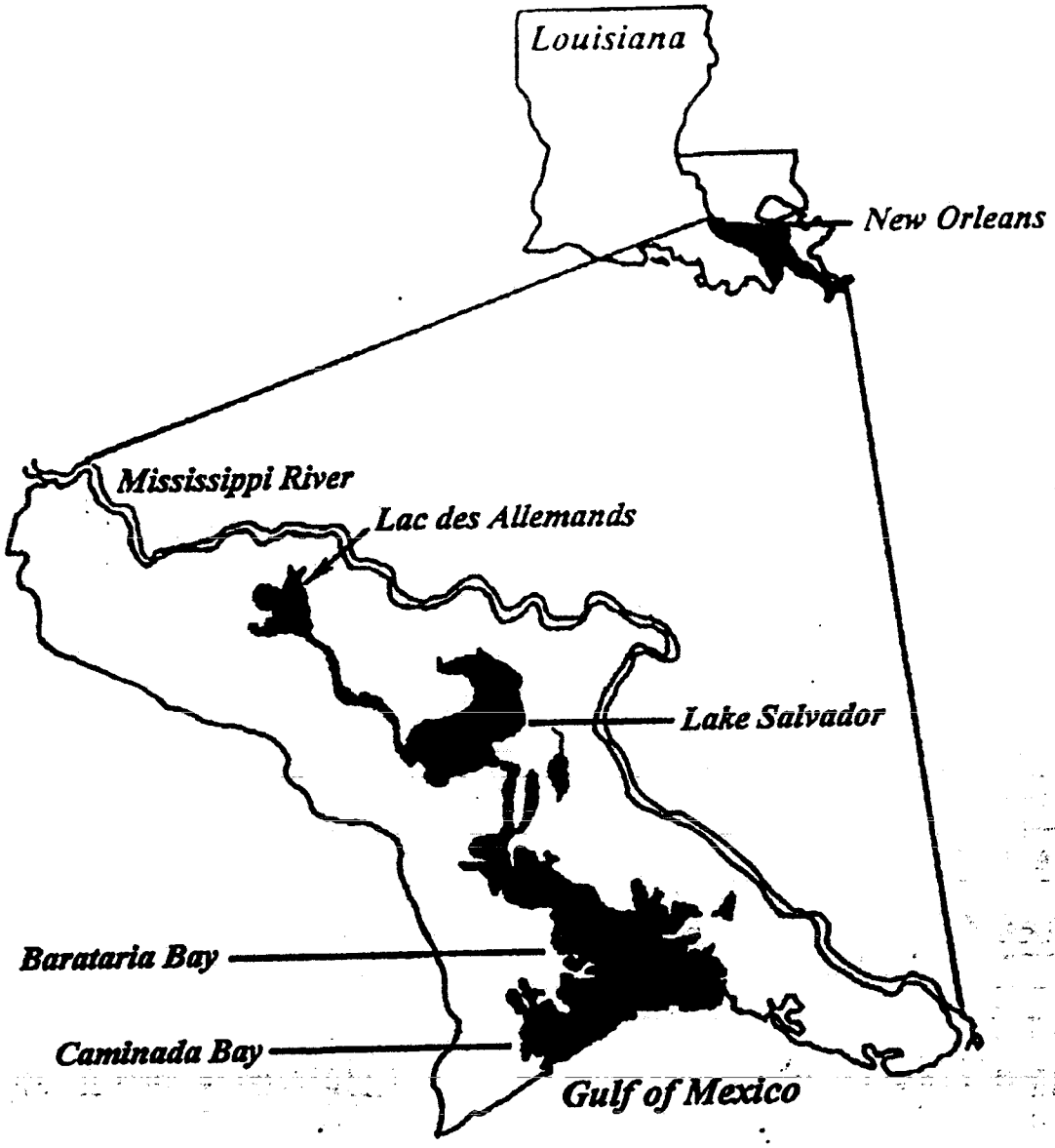
Louisiana
New Orleans
Mississippi River
Lac des Allemands
Lake Salvador
Barataria Bay
Caminada Bay
Gulf of Mexico

Figure 1.

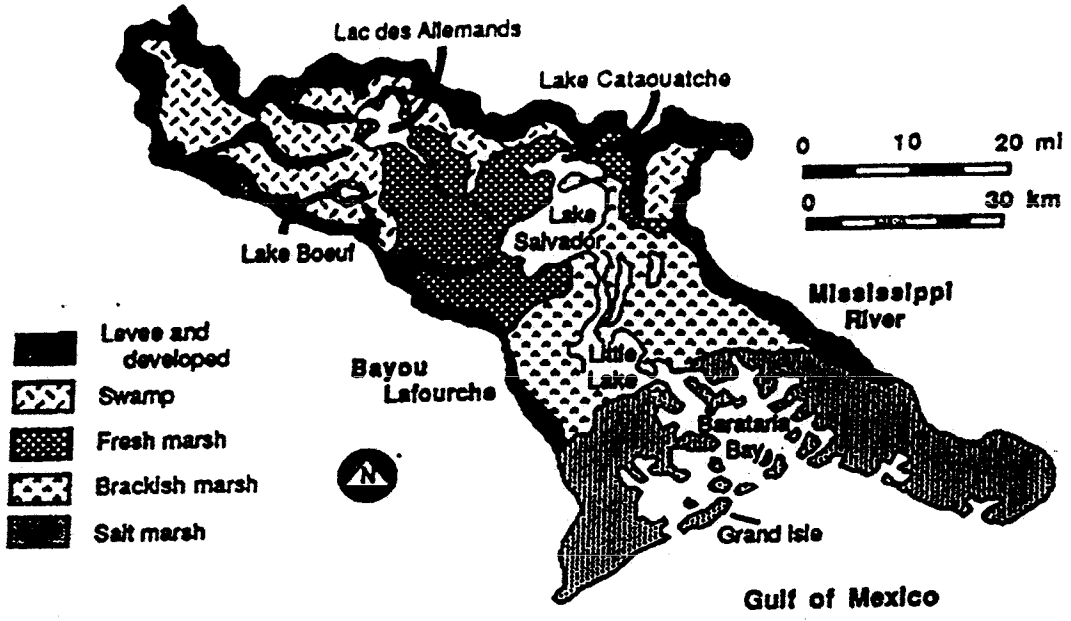
Lac des Allemands
Lake Cataouatche
0 10 20 mi
0 30 km
Lake Salvador
Lake Boeuf
Mississippi River
Levee and developed
Swamp
Fresh marsh
Brackish marsh
Salt marsh
Bayou Lafourche
Little Lake
Barataria Bay
Grand Isle
Gulf of Mexico

Figure 2.

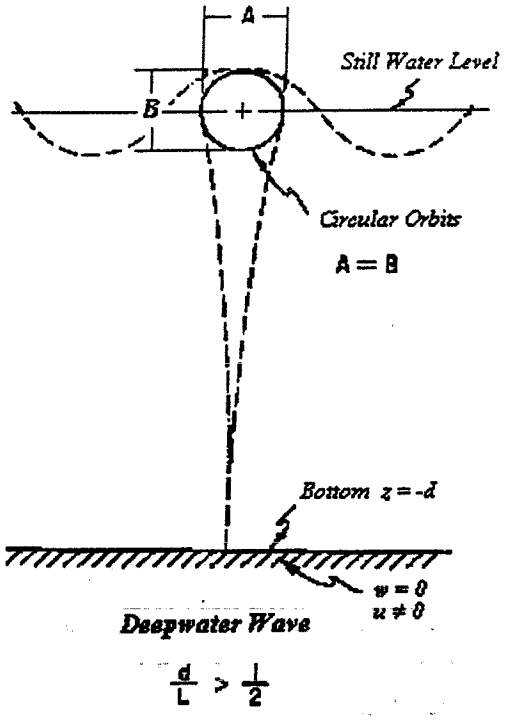
A
B
Still Water Level
Circular Orbits
A = B
Bottom z = -d
w = 0
u ≠ 0
Deepwater Wave
d/L > 1/2

Figure 3.

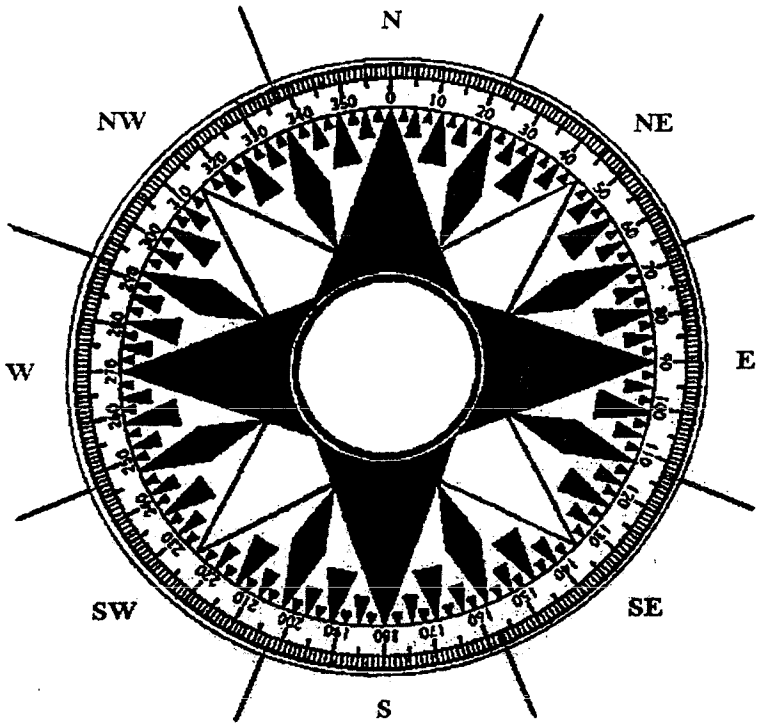

Figure 4.

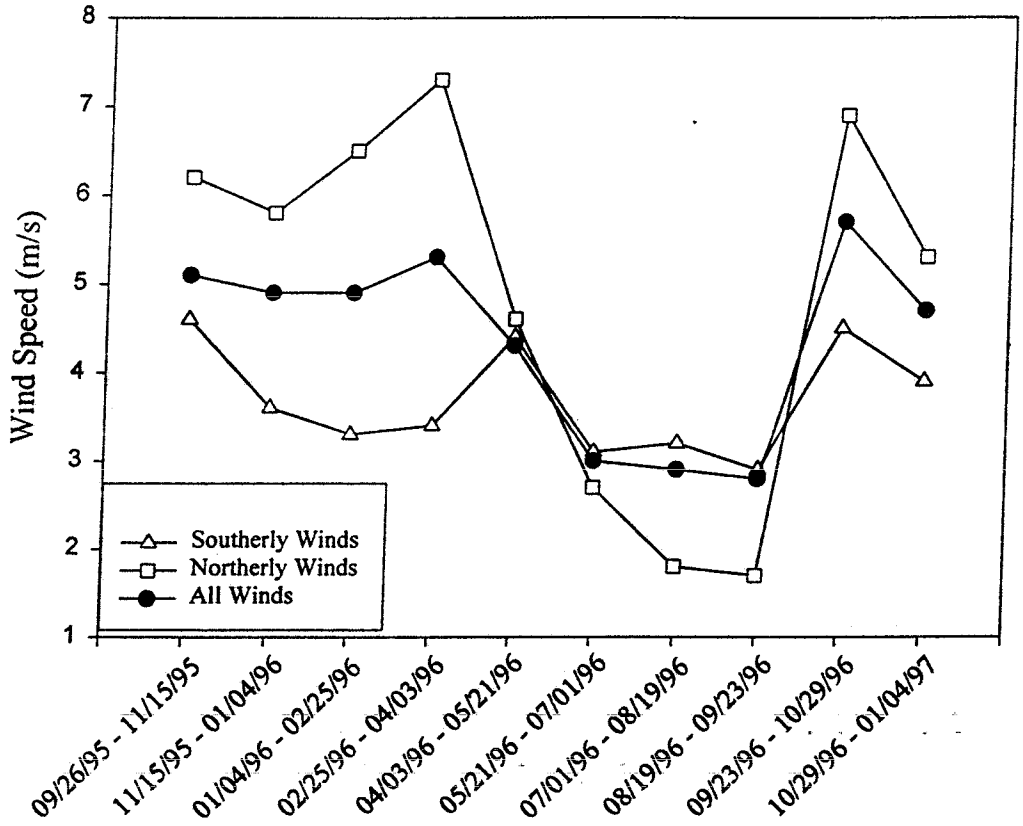
Wind Speed (m/s)
8
7
6
5
4
3
2
1
Southerly Winds
Northerly Winds
All Winds
09/26/95 - 11/15/95
11/15/95 - 01/04/96
01/04/96 - 02/25/96
02/25/96 - 04/03/96
04/03/96 - 05/21/96
05/21/96 - 07/01/96
07/01/96 - 08/19/96
08/19/96 - 09/23/96
09/23/96 - 10/29/96
10/29/96 - 01/04/97

Figure 5.

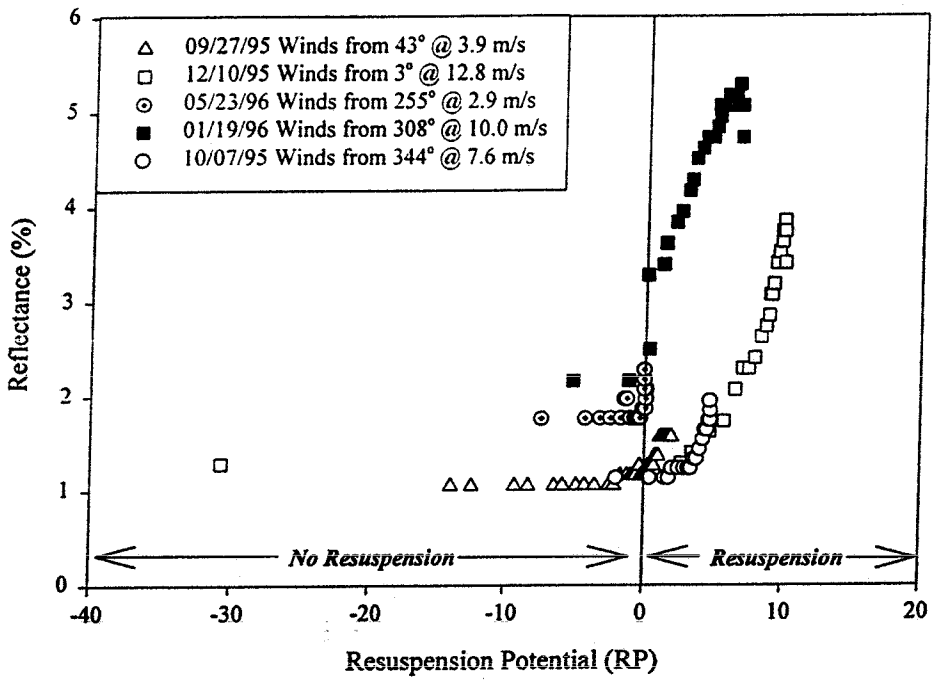
09/27/95 Winds from 43° @ 3.9 m/s
12/10/95 Winds from 3° @ 12.8 m/s
05/23/96 Winds from 255° @ 2.9 m/s
01/19/96 Winds from 308° @ 10.0 m/s
10/07/95 Winds from 344° @ 7.6 m/s
Reflectance (%)
No Resuspension
Resuspension
Resuspension Potential (RP)

Figure 6.

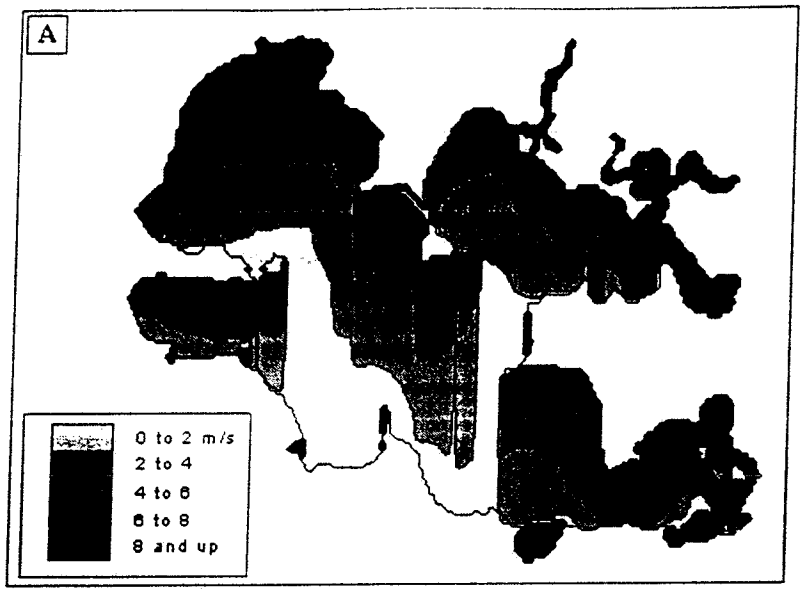
A
0 to 2 m/s
2 to 4
4 to 6
6 to 8
8 and up

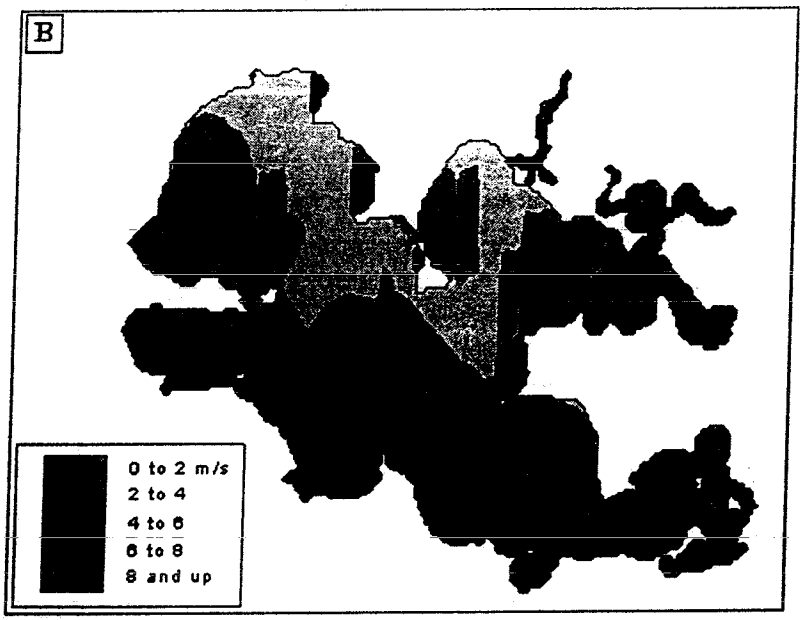
B
0 to 2 m/s
2 to 4
4 to 6
6 to 8
8 and up

Figure 7.

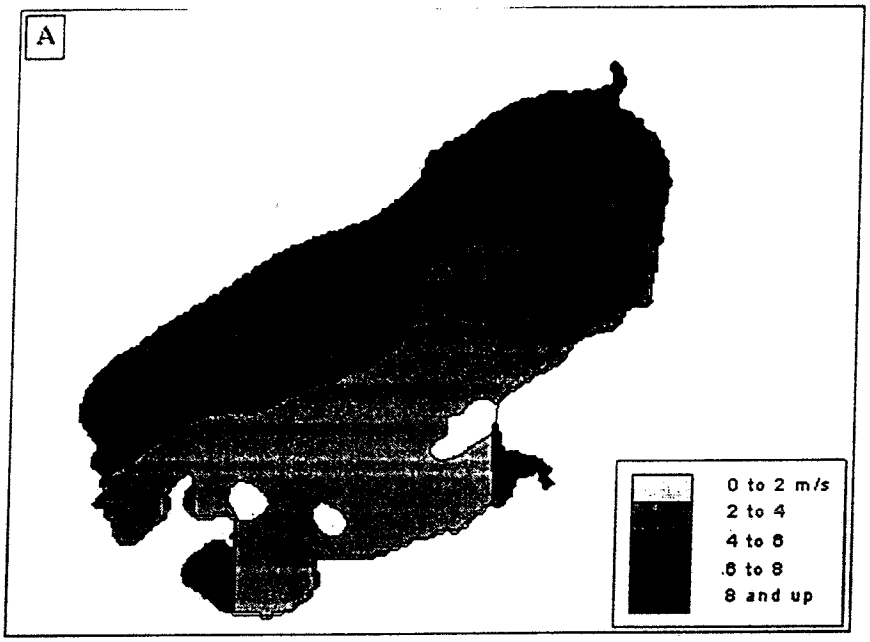
A
0 to 2 m/s
2 to 4
4 to 6
6 to 8
8 and up

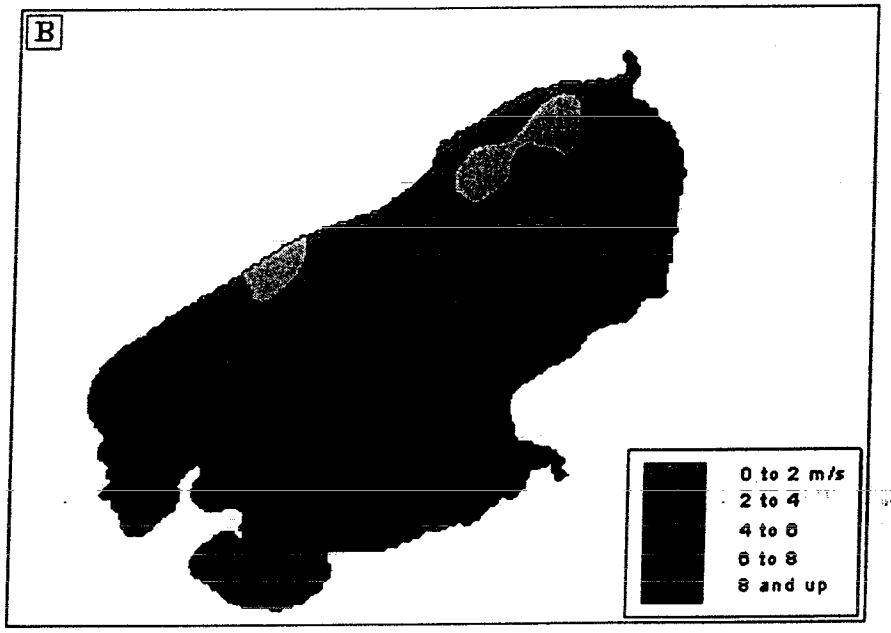
B
0 to 2 m/s
2 to 4
4 to 6
6 to 8
8 and up

Figure 8.

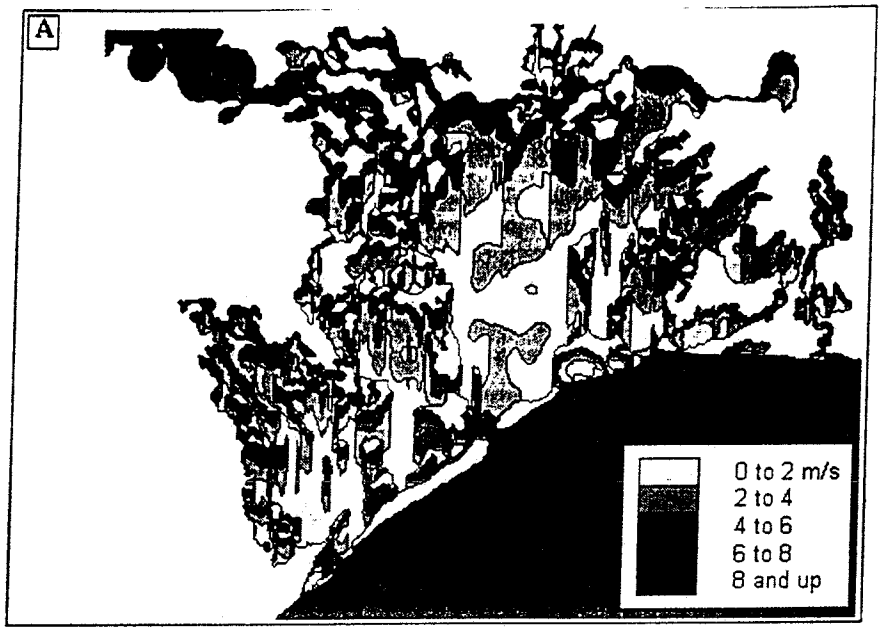
A
0 to 2 m/s
2 to 4
4 to 6
6 to 8
8 and up

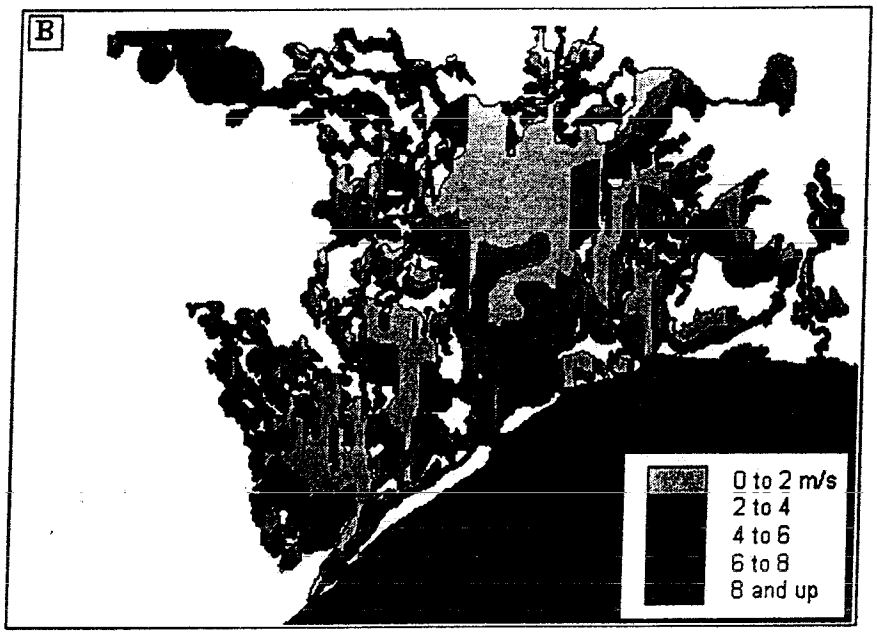
B
0 to 2 m/s
2 to 4
4 to 6
6 to 8
8 and up

Figure 9.

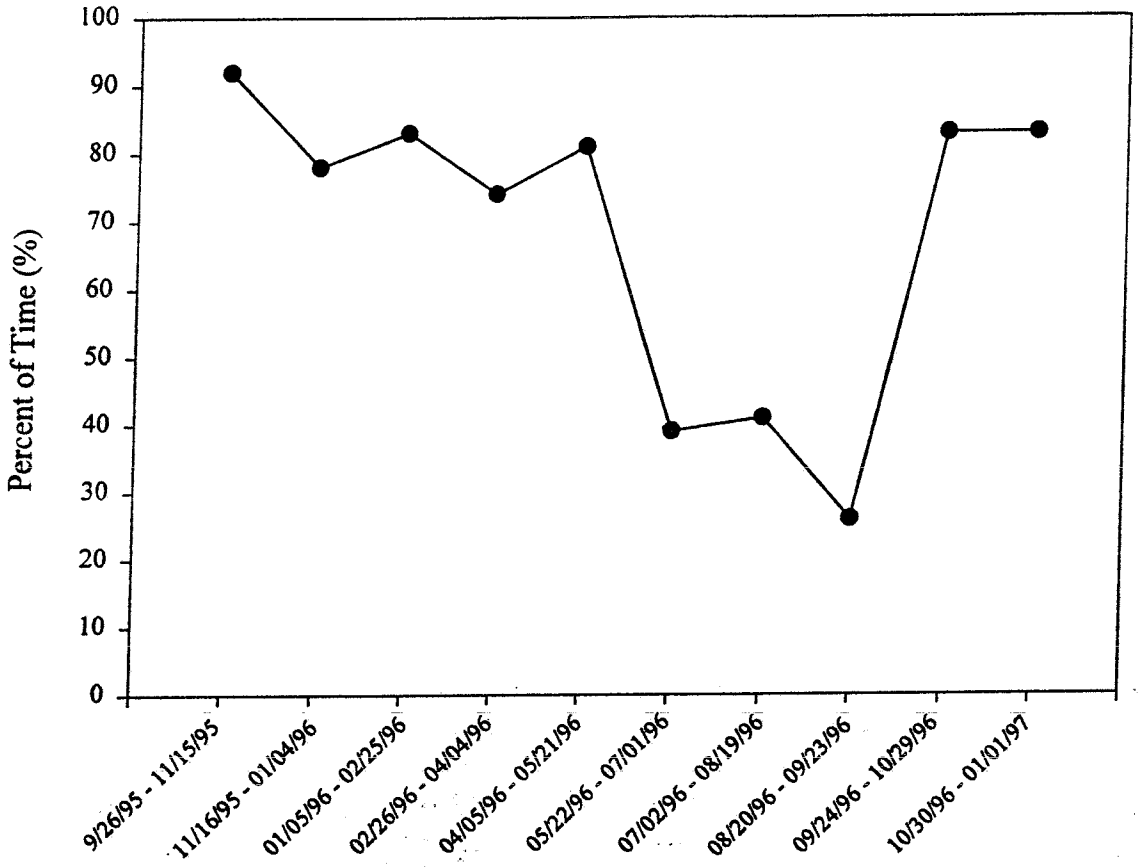
Percent of Time (%)
100
90
80
70
60
50
40
30
20
10
0
9/26/95 - 11/15/95
11/16/95 - 01/04/96
01/05/96 - 02/25/96
02/26/96 - 04/04/96
04/05/96 - 05/21/96
05/22/96 - 07/01/96
07/02/96 - 08/19/96
08/20/96 - 09/23/96
09/24/96 - 10/29/96
10/30/96 - 01/01/97

Figure 10.

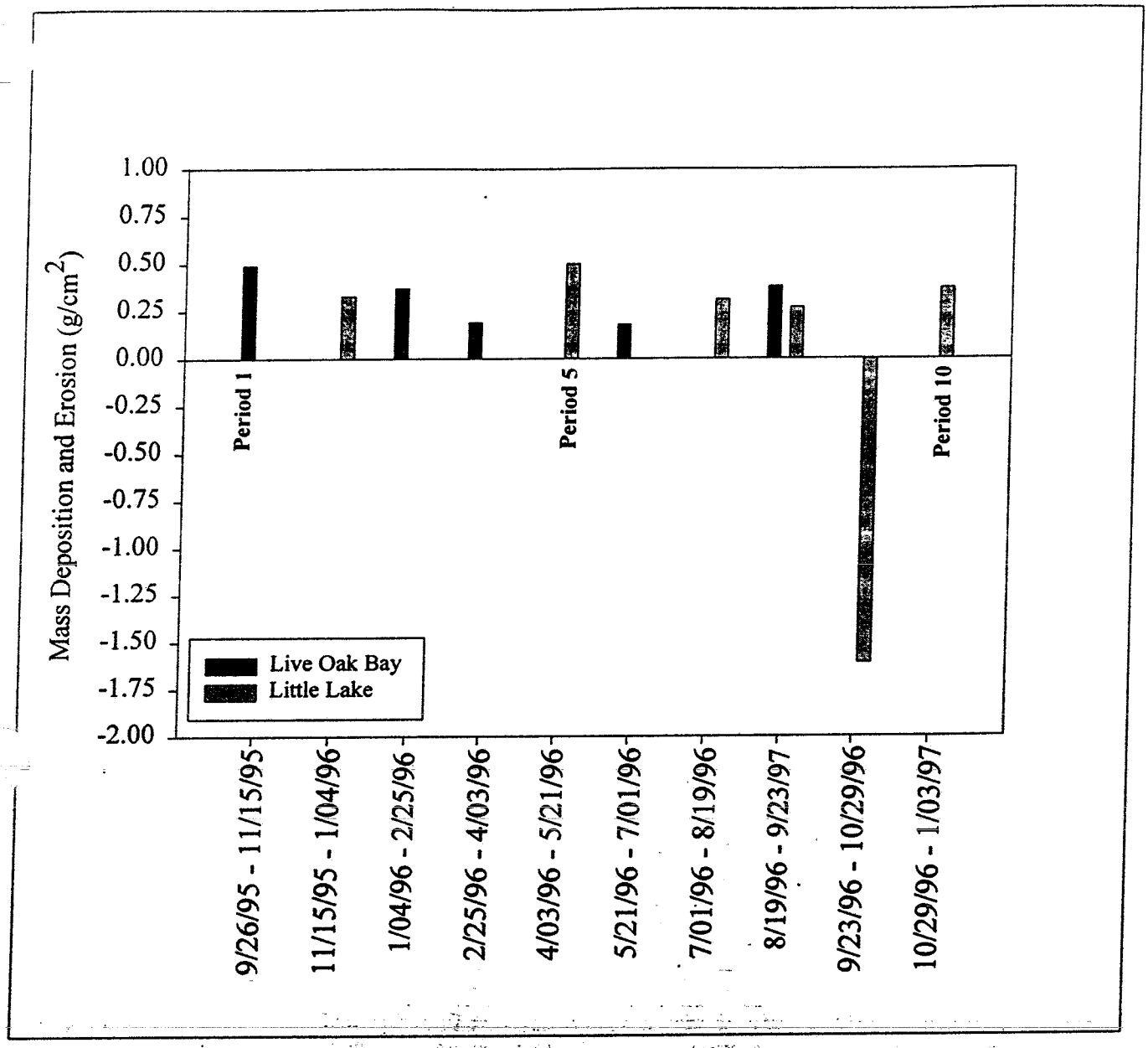
Mass Deposition and Erosion (g/cm2)
1.00
0.75
0.50
0.25
0.00
-0.25
-0.50
-0.75
-1.00
-1.25
-1.50
-1.75
-2.00
Period 1
Period 5
Period 10
Live Oak Bay
Little Lake
9/26/95 - 11/15/95
11/15/95 - 1/04/96
1/04/96 - 2/25/96
2/25/96 - 4/03/96
4/03/96 - 5/21/96
5/21/96 - 7/01/96
7/01/96 - 8/19/96
8/19/96 - 9/23/97
9/23/96 - 10/29/96
10/29/96 - 1/03/97

Figure 11.

Figure Captions

Figure 1. Location of the Barataria Basin with major water bodies identified.

Figure 2. Habitat map of the Barataria Basin (from Conner and Day, 1987).

Figure 3. Water particle motion for deepwater waves (from the U.S. Army Coastal Engineering Research Center, 1977).

Figure 4. Wind data grouped into eight directions according to the diagram above.

Figure 5. Mean daily wind speeds for each time period. Northerly and southerly winds include westerly and easterly components (i.e. N, NW, NE and S, SW, SE).

Figure 6. Model prediction of resuspension potential (RP) vs. AVHRR channel 1 reflectance. Reflectance (or water turbidity) exhibits good agreement with model estimates of when resuspension should occur (i.e. RP values of 0 and above).

Figure 7. Isopleths of U_c (m/s) in Little Lake. Isolines represent the windspeed required to induce resuspension for a north wind (360°) (A) and south wind (180°) (B). Each contour represents the region that would be subject to resuspension at the indicated wind speed.

Figure 8. Isopleths of U_c (m/s) in Lake Salvador. Isolines represent the windspeed required to induce resuspension for a north wind (360°) (A) and a south wind (180°) (B). Each contour represents the region that would be subject to resuspension at the indicated windspeed.

Figure 9. Isopleths of U_c (m/s) in the lower Barataria Basin. Isolines represent the wind speed required to induce resuspension for a north wind (360°) (A) and a south wind (180°) (B). Each contour represents the region that would be subject to resuspension at the indicated wind speed. The black regions in the lower right hand corners of this figure (i.e. below the islands) are not represented by the legend.

Figure 10. Percentage of time during each study period that the average daily wind speed was equal to or greater than 4 m/s.

Figure 11. Seasonal particle transport (deposition and erosion) rates to bottom sediments.

Table 1. Directional wind energy distribution for each period of this study. Winds were sorted according to Figure 5. Bold numbers at the bottom represent directional totals and percent of total wind energy for this study.

Period	NW	N	NE	E	SE	S	SW	W	Σ energy (m^2s^{-2})
1	6.1	32.3	37.5	10.5	6.9	2.2	2.1	2.4	54358
2	8.8	38.8	17.6	8.3	5.4	5.8	3.1	12.2	40488
3	27.7	29.2	9.1	8.1	9.3	6.0	6.2	4.3	44884
4	15.6	35.4	16.0	5.7	9.0	4.2	3.1	11.0	38882
5	9.0	16.3	8.6	8.3	44.0	10.4	2.0	1.3	31582
6	7.2	5.4	5.9	11.1	21.1	29.5	10.2	9.7	14365
7	10.8	4.3	4.1	10.7	17.5	16.1	16.8	19.7	19159
8	7.0	5.6	10.5	30.8	7.5	11.8	18.9	7.8	13759
9	5.6	23.5	49.9	8.7	7.5	4.0	0.1	0.8	37022
10	15.5	19.6	17.5	15.5	8.2	9.2	4.7	9.7	48219
Total	**41833.4**	**85806.3**	**70521.8**	**36118.4**	**41653.1**	**26017.7**	**16604.1**	**24076.1**	**342718.0**
%	**12.2**	**25.0**	**20.6**	**10.5**	**12.2**	**7.6**	**4.8**	**7.0**	**100**

Table 2. Directional wind energy distribution for 1990 through 1996. Winds were sorted according to Figure 5. Bold numbers at the bottom represent directional totals and percent of total wind energy during the seven-year period.

Year	NW	N	NE	E	SE	S	SW	W	Σ energy (m^2s^{-2})
1990	12.0	22.8	14.8	18.6	15.9	6.8	3.8	5.2	253181.1
1991	8.6	15.1	21.4	20.5	16.3	8.7	4.4	5.1	296282.4
1992	10.0	18.2	24.7	14.9	12.0	6.8	6.4	6.8	269045.5
1993	14.0	20.1	18.9	16.7	10.6	6.7	4.6	8.3	285808.7
1994	11.6	20.8	22.5	15.8	10.5	7.7	6.0	5.2	274577.6
1995	10.2	24.0	20.7	12.9	11.6	9.1	4.8	6.8	315524.1
1996	15.1	20.1	17.1	10.8	14.3	9.0	5.8	7.9	297216.9
Totals*	**231694**	**401456**	**399265**	**311833**	**259065**	**157042**	**101882**	**129507**	**1991636.2**
%	**11.6**	**20.2**	**20.0**	**15.7**	**13.0**	**7.9**	**5.1**	**6.5**	**100.0**

Table 3. Cumulative bottom sediment resuspended in Little Lake. The numbers under the wind direction headings represent the percent of bottom sediments (on an areal basis) that are resuspended at the wind speed in the left column. The percentages are cumulative as wind speed increases.

		Bottom Sediment Resuspension (%)						
U_c (m/s)	NW (315°)	N (360°)	NE (45°)	E (90°)	SE (135°)	S (180°)	SW (225°)	W (270°)
2	18.4	18.4	6.3	23.1	19.5	21.1	10.6	24.2
4	47.8	50.2	36.0	59.3	48.2	50.7	36.6	59.7
6	62.0	68.2	58.7	73.1	62.5	65.4	54.6	72.5
8	71.4	76.5	70.3	79.6	71.0	74.2	67.1	79.7
10	78.1	81.9	77.1	83.9	76.8	79.6	74.5	84.3

Table 4. Cumulative bottom sediment resuspended in Lake Salvador. The numbers under the wind direction headings represent the percent of bottom sediments (on an areal basis) that are resuspended at the wind speed in the left column. The percentages are cumulative as wind speed increases.

		Bottom Sediment Resuspension (%)						
U_c (m/s)	NW (315°)	N (360°)	NE (45°)	E (90°)	SE (135°)	S (180°)	SW (225°)	W (270°)
2	0.0	2.6	1.9	2.9	0.9	4.8	6.9	2.9
4	32.0	53.0	60.6	58.6	30.3	55.2	56.5	61.6
6	53.7	72.3	74.8	74.2	54.3	71.7	72.0	77.2
8	68.6	80.8	81.5	82.4	68.6	79.8	79.8	83.7
10	76.9	85.2	85.6	86.5	76.1	84.2	84.3	87.4

Table 5. Cumulative bottom sediment resuspended (%) in the lower Barataria Basin. The numbers under the wind direction headings represent the percent of bottom sediments (on an areal basis) that are resuspended at the wind speed in the left column. The percentages are cumulative as wind speed increases.

		Bottom Sediment Resuspension (%)						
U_c (m/s)	NW (315°)	N (360°)	NE (45°)	E (90°)	SE (135°)	S (180°)	SW (225°)	W (270°)
2	16.6	28.4	18.3	29.3	20.3	32.4	23.2	28.9
4	47.5	62.6	50.6	57.1	48.4	59.4	48.7	57.2

National Aeronautics and
Space Administration

John C. Stennis Space Center
Stennis Space Center, MS 39529-6000

Reply to Attn of RA50

May 3, 1999

TO: Distribution

FROM: RA50/SSC Interagency Agreements (IA) Coordinator
THRU RA50/Chief, Information Management Division

SUBJECT: Request for Status of SSC IAs

The following SSC IAs have expired or will expire in 1999. Please provide a status for each expired agreement. If expired agreements will be renewed, please submit new agreements immediately for concurrence and execution; if current agreements will be renewed, please submit 90 days prior to the expiration date for completion of renewal process prior to expiration.

AAOO - NASA/SSC Exchange Concessionaire Agreements – Review Annually
- SSC Recreation Association – 6/98
- Barber Shop – 8/98
- The Cobbler Shoe Repair – 3/99
- Stennis Child Development Center – 3/99
- Hancock Bank – 4/99
- Corporate Cleaners – Annual Review
- Service Station – Annual Review
- Snack Bar – Annual Review

AA10 - Gulf Coast Education Initiative Consortium – 9/98
- Jackson State University – 10/98
- MS Institution of Higher Learning – Annual Review

RA00 - MSFC/SSC for NASA ADP Consolidation Center – 4/98
- Hancock County – MS Board of Supervisors/
  Patrol Service in Buffer Zone – 9/98
- St. Tammany Parish Mosquito Control – 9/98
- Hancock County Mosquito Control – 9/98
- Naval Support Activity – Specia
- Mutual Aid – Fire Dept (10 Agre

SA00 - Surveys Unlimited Research Ass

TA00 - LA State Dept. of Economic Devel
- MS Dept of Economic & Communit

I believe that this is Marco's.

's

REPORT DOCUMENTION PAGE

Form Approved
OMB No. 0704-0188

1. AGENCY USE ONLY *(Leave blank)*	2. REPORT DATE	3. REPORT TYPE AND DATES COVERED
	1999	Final

4. TITLE AND SUBTITLE

Wind induced sediment resuspension in a microtidal estuary

5. FUNDING NUMBERS

PR

6. AUTHOR(S)

J.G. Booth, R.L. Miller, B.A. McKee and R.A. Leathers

7. PERFORMING ORGANIZATION NAME(S) AND ADDRESS(ES)

NASA/ESSO
Building 1100 SA00
Stennis Space Center, MS 39529

8. PERFORMING ORGANIZATION REPORT NUMBER

SE-1999-05-00018-SSC

9. SPONSORING/MONITORING AGENCY NAME(S) AND ADDRESS(ES)

10. SPONSORING/MONITORING AGENCY REPORT NUMBER

11. SUPPLEMENTARY NOTES

To be published in the peer reviewed scientific journal Continental Shelf Research

12a. DISTRIBUTION/AVAILABILITY STATEMENT

Publicly Available

12b. DISTRIBUTION CODE

13. ABSTRACT ***(Maximum 200 words)***

Abstract
Bottom sediment resuspension frequency, duration and extent (% of bottom sediments affected) were characterized for the fifteen month period from September 1995 to January 1997 for the Barataria Basin, LA. An empirical model of sediment resuspension as a function of wind speed, direction, fetch and water depth was derived from wave theory. Water column turbidity was examined by processing remotely sense radiance information from visible and near-IR AVHRR imagery. Based on model predictions, wind induce resuspension occurred during all seasons of this study. Seasonal characteristics for resuspension reveal tha late fall, winter and early spring are the periods of most frequent and intense resuspension. Model predictions of the critical wind speed required to induce resuspension indicate that winds of 4 m/s (average over all wind directions) resuspend approximately 50% of bottom sediments in the water bodies examined. Winds of this magnitude (4 m/s) occurred for 80 % of the time during the late fall, winter and early spring and for approximately 30 % of the time during the summer. More than 50% of the bottom sediments are resuspended throughout the year, indicating the importance of resuspension as a process affecting sediment and biogeochemical fluxes in the Barataria Basin.

14. SUBJECT TERMS	15. NUMBER OF PAGES
esuspension, Resuspended sediments, Estuarine Dynamics, Remote Sensing	42
	16. PRICE CODE

17. SECURITY CLASSIFICATION OF REPORT	18. SECURITY CLASSIFICATION OF THIS PAGE	19. SECURITY CLASSIFICATION OF ABSTRACT	20. LIMITATION OF ABSTRACT